J. Cent. South Univ. (2023) 30: 786−799
DOI: https://doi.org/10.1007/s11771-023-5280-1

Springer

Intensive carbon combustion in sintering packed bed via steam spraying: An experimental study on carbon monoxide emission reduction

SUN Cheng-feng(孙成烽)[1], ZHOU Xuan-geng(周炫庚)[1], LI Gang(李刚)[1],
WANG Yue-fei(王跃飞)[2], XIE Xue-rong(谢学荣)[2], LYU Xue-wei(吕学伟)[1], XU Jian(徐健)[1]*

1. College of Materials Science and Engineering, Chongqing University, Chongqing 400044, China;
2. Baoshan Iron & Steel Co., Ltd., Shanghai 201900, China

© Central South University 2023

Abstract: Improving the combustion efficiency of solid fuels is important for reducing carbon monoxide emissions in the iron ore sintering process. In this paper, the surface steam spraying technology is introduced in the sintering process based on the auxiliary combustion effect of steam on coke, and its potential to reduce carbon monoxide emissions is demonstrated. Thermogravimetric analysis experiments of coke breeze in air and air-steam mixed atmosphere are carried out, and the results show that the introduction of steam can reduce the concentration of carbon monoxide in the exhaust gas from 183×10^{-6} to 78×10^{-6}. At the same time, the mechanisms of carbon monoxide emission reduction by surface steam spraying technology are analyzed from the thermodynamic and kinetic perspectives. Then, a series of laboratory-scale sintering pot tests are carried out under no spraying operation, interval spraying operation, and continuous spraying operation. The results indicate that both interval and continuous spraying operations can reduce carbon monoxide emissions. The optimal mode of steam spraying under the present experimental conditions is continuously spraying for 13 min at a volume rate of 0.053 m^3/min. Compared with no spraying, the average carbon monoxide concentration in the exhaust gas is reduced from 7565×10^{-6} to 6231×10^{-6}, and total carbon monoxide emissions for per ton sinter are reduced from 13.46 m^3/t to 9.51 m^3/t.

Key words: sintering; carbon combustion; steam spraying; carbon monoxide; emission reduction

Cite this article as: SUN Cheng-feng, ZHOU Xuan-geng, LI Gang, WANG Yue-fei, XIE Xue-rong, LYU Xue-wei, XU Jian. Intensive carbon combustion in sintering packed bed via steam spraying: An experimental study on carbon monoxide emission reduction [J]. Journal of Central South University, 2023, 30(3): 786 − 799. DOI: https://doi. org/10.1007/s11771-023-5280-1.

1 Introduction

Environmental issues, including air pollution, environmental degradation, global warming, ozone depletion, and acid rain, are largely related to uncontrolled and excessive use of natural resources [1 − 4]. Both governments and industries are responsible for reducing emissions from human activities through strict regulation [5 − 9]. Carbon monoxide (CO), one of the most common air pollutants, is recognized as a significant threat to human health [10] and plays an essential role in various photochemical oxidation processes in the atmosphere [11], such as the formation of tropospheric ozone [12]. CO is mainly produced

Foundation item: Project(cstc2021ycjh-bgzxm0165) supported by the Natural Science Foundation of Chongqing, China; Project (BWLCF202102) supported by the China Baowu Low Carbon Metallurgy Innovation Foundation; Project(CYB20007) supported by the Graduate Scientific Research and Innovation Foundation of Chongqing, China
Received date: 2022-06-16; **Accepted date:** 2023-02-09
Corresponding author: LYU Xue-wei, PhD, Professor; E-mail: lvxuewei@cqu.edu.cn; ORCID: https://orcid/0000-0002-1985-4642; XU Jian, PhD, Professor; E-mail: jxu@cqu.edu.cn; ORCID: https://orcid/0000-0002-7565-9665

from incomplete combustion of fossil fuels [13] due to insufficient oxygen supply or insufficient mixing [14]. As the second-largest CO emitting industry after the automobile industry [15], the steel production accounts for 17.4% of CO emissions [16−17], while iron ore sintering processes account for 34.4% by burning approximately 50 kg fossil fuels per ton sinter [18 − 21]. The rate of CO emissions from combustion systems depends on the combustion efficiency of fossil fuels [22 − 23]. The key to reducing CO emissions is to improve fuel combustion efficiency [14, 24], i. e. to further oxidize CO into carbon dioxide (CO_2), thereby reducing fuel consumption.

To date, intensive research has been conducted by experimental [25−29] and numerical studies [30−33] to find cost-effective methods to reduce CO emissions in the sintering process. Specifically, emission reduction strategies can be broadly divided into two categories. On the one hand, CO emission reduction can be achieved by reducing the addition of coke breeze, and a series of practical technologies have been developed, such as ultra-thickness bed sintering technology [34 − 36], coke breeze segregation [37 − 39], biomass fuel substitution [25, 27, 40−41], return fines embedding technology [42] and composite agglomeration technology [43 − 44]. Ultra-thickness bed sintering technology has been widely used to reduce fuel consumption due to the advantage of energy storage effect. It is noted that every 100 mm increase in bed height can not only improve the mechanical strength and yield of the sinter, but also reduce energy consumption by approximately 10 kgce/t [45]. Meanwhile, a series of comprehensive technologies to ensure the bed permeability are essential [46−47]. Due to the increased melting quantity index in the upper burden region, CHENG et al [30] proposed that fuel segregation with multi-layers can achieve a more reasonable heat pattern distribution, which can subsequently reduce CO concentration in exhaust gas from 0.8% to 0.6%. Biomass fuel, which is characterized by higher chemical activity than coke breeze, is the potentially appropriate alternative to coke breeze for the sake of controlling CO emissions [48]. KAWAGUCHI et al [49] found that the combustion efficiency of biomass-char was faster than that of coke, and LEGEMZA et al [50] demonstrated that the average concentration of CO decreased with the addition of biomass-char by approximately 30%. However, a higher replacement proportion has an adverse impact on the quality of the sinter. GAN et al [51] found that when the proportion of biomass replacing coke exceeded 40%, both sinter yield and tumble index decreased. In addition, the latest research results showed that the improvement of bed permeability through the return fines embedding technology not only strengthened the quality and yield of the sinter, but also reduced fuel consumption by 16% [52]. Process control has also become an effective way to reduce CO emissions. Therefore, innovative technologies developed in recent decades have been generally accepted and put into production in sintering plants, such as sintering flue gas recirculation [53 − 56], stand-support sintering [45, 57 − 58], gaseous fuel injection [59 − 62] and double-layer ignition sintering [34, 63]. It was reported that CO emissions could be reduced by 22.06% with the application of sintering flue gas recirculation technology [25]. At the same time, this technology inevitably brought changes to gas flow and conditions across the bed [64]. WANG et al [58] found that the stand-support reduced CO concentration by 44.4% and increased production by 17.4%. Although various technologies have been developed to reduce CO emissions, huge operational challenges, high retrofit costs, and additional pollutants limit their large-scale application.

As we all know, humidified combustion has been applied to various fields such as internal combustion engines [65], coal slurry [66], coal combustion [67] and coal gasification [68], because it can improve the combustion efficiency of fuel. However, super-humid in the combustion system will affect combustion stability and exhaust gas emissions [69]. This can lead to unstable, incomplete combustion, which will negatively affect combustion efficiency and increase CO emissions. Therefore, it is very important to figure out the appropriate degree of humidification of the combustion system to improve combustion efficiency. Surface steam spraying technology is employed to investigate the potential for CO emission reduction in this paper. First, the thermodynamic response to coke combustion before and after spraying steam is compared, and the mechanistic analysis of CO emission reduction is

provided. Second, through thermogravimetric analysis experiments, it is proved that the coke combustion efficiency in the mixed atmosphere of air and steam is higher than that in the air atmosphere, which can further reduce CO emissions. Third, laboratory-scale sintering pot tests are conducted with three spraying patterns, namely no spraying pattern, interval spraying pattern, and continuous spraying pattern, and the composition and temperature distributions of exhaust gas and the comparative results of sinter yield and quality are quantitatively described. The results show that both the interval and the continuous spraying patterns can achieve the goal of reducing CO emissions, while the continuous spraying operation has a more significant emission reduction effect at the same steam volume rate.

2 Experimental

2.1 Properties of coke breeze

The coke breeze is used as the fossil fuel in the sintering process. Its proximate analysis results are summarized in Table 1, while its appearance and particle size distribution are shown in Figure 1.

2.2 Pyrolysis analysis of coke breeze in humidified air

The coke breeze is subjected to pyrolysis analysis in the thermogravimetric analyzer (Setsys Evo TG-DTA1750). 7.1 mg weighed samples are heated from ambient temperature to 1000 ℃ at a heating rate of 20 ℃/min in humidified air, which is a mixture of air and steam generated from the humidity generator (Setaram Wetsys). The humidified air has a humidity of about 45%, and its flow rate is 40 mL/min. Meanwhile, the exhaust gas composition is analyzed through Fourier infrared flue gas analyzer (Antaris IGS).

2.3 Combustion emission analysis of coke breeze with steam spraying in packed bed

As shown in Figure 2, a laboratory-scale sintering pot with a steam sprayer is used to simulate the practical sintering process. The raw materials are first mixed and granulated in a rotating granulator with a diameter of 945 mm and a length of 1200 mm for 10 min and 15 min, respectively. Subsequently, the granules obtained by the granulator are charged into the sintering pot with a height of 800 mm and a diameter of 300 mm. The coke breeze on the surface is initially ignited by an ignitor to maintain the ignition temperature (1323 K) for 2 min with a negative suction pressure of 8 kPa, and then the combustion front and sprayed steam move downwards with a negative suction pressure of 10 kPa.

Throughout the sintering process, an infrared flue gas analyzer and thermocouple are used to monitor exhaust gas composition and temperature. In addition, the sinter cake is subjected to yield and quality evaluation with formulas in Table 2.

Table 1 Proximate analysis results of coke breeze

w(ash)/%	*w*(moisture)/%	*w*(volatile)/%	*w*(fixed carbon)/%	Calorific value/(MJ·kg^{-1})
12.64	0.53	2.24	84.69	27.43

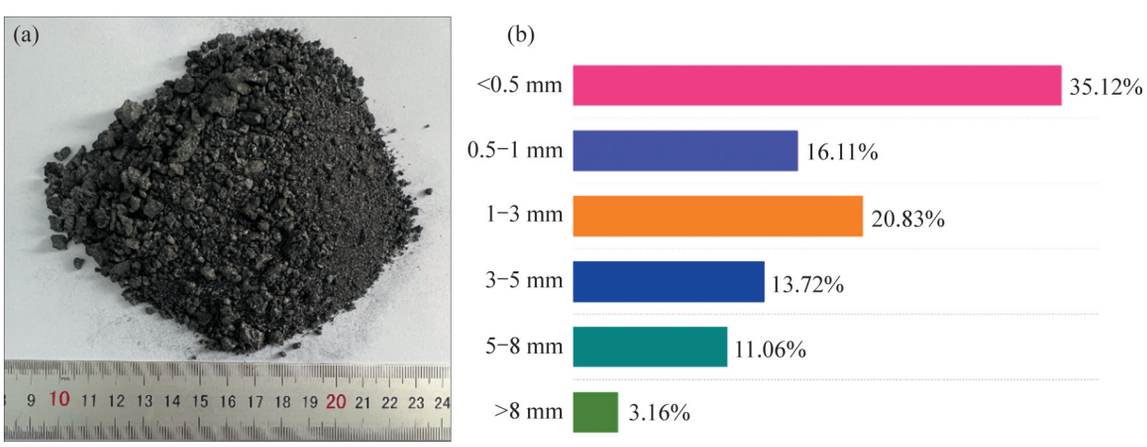

Figure 1 (a) Appearance and (b) particle size distribution in mass fraction of coke breeze

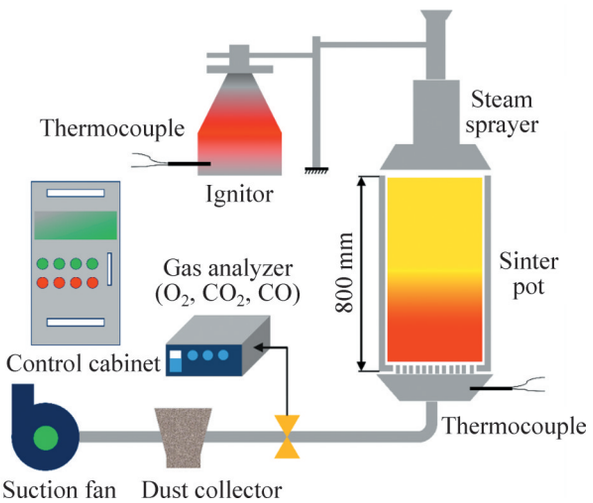

Figure 2 Schematic diagram of sintering pot test with surface steam spraying technology

Table 2 Formulas used for determining yield and quality indices of sinter

Evaluation index	Formula	Note
Tumbler index	$I_T = \frac{m_{6.3\,mm+}}{m_0} \times 100\%$	$m_{6.3\,mm+}$: mass of sinters with size greater than 6.3 mm after tumbling, kg; m_0: mass of samples, kg
Shatter index	$I_S = \frac{m_{10\,mm+}}{m_0} \times 100\%$	$m_{10\,mm+}$: mass of sinters with size greater than 10 mm after shatter, kg; m_0: mass of samples, kg
Productivity	$\gamma = \frac{m_a}{m_w} \times 100\%$	m_a: mass of sinter cake, kg; m_w: mass of sinter mixtures, kg
Sinter yield	$Y = \frac{m_{5\,mm+}}{m_a} \times 100\%$	$m_{5\,mm+}$: mass of sinters with size greater than 5 mm, kg

Iron ore fines, fluxes (including dolomite, limestone, and quicklime), fuels and return fines are used as raw materials, which are offered by Baosteel, Shanghai. The chemical composition of raw materials is given in Table 3. The weighed raw materials are mixed with 8.0% moisture, and approximately 100 kg raw materials including 62.15% iron ore fines, 9.01% fluxes, 3.38% coke breeze, and 25.46% return fines are charged into the pot after granulation.

Three different spraying patterns, namely no spraying (NS), interval spraying (IS), and continuous spraying (CS) shown in Figure 3 are

Table 3 Chemical composition of raw materials wt%

Material	TFe	SiO_2	CaO	MgO	Al_2O_3	LOI
Iron ore fines	59.88	4.58	1.05	0.24	1.73	8.92
Dolomite	0.36	3.56	18.34	29.43	1.03	45.93
Limestone	0.35	2.08	52.25	3.21	1.03	42.32
Quicklime	0.32	1.83	83.30	0.58	0.33	13.03
Coke breeze	0.45	3.96	1.04	0.13	4.60	84.62
Return fines	57.44	5.54	9.74	1.33	1.99	2.15

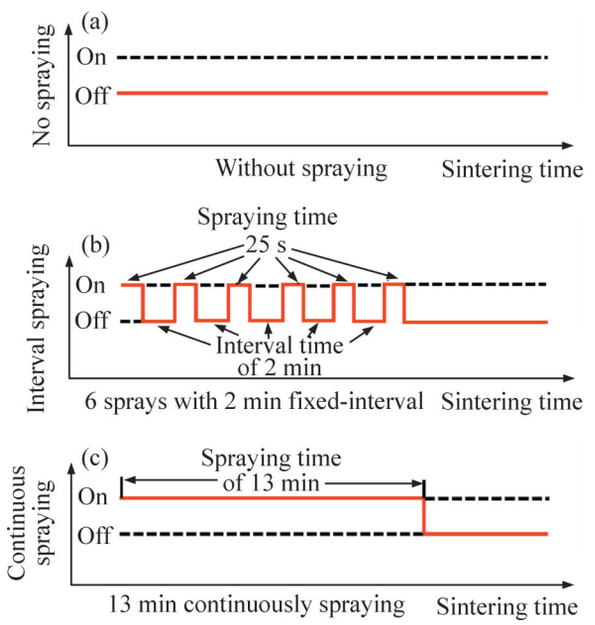

Figure 3 Detailed explanations of three spraying patterns: (a) NS; (b) IS; (c) CS

employed in this work to investigate the influence of the spraying pattern on the sintering performance. In addition, the IS pattern sprays steam at the steam volume rates of 0.025 (denoted by IS1) and 0.053 (denoted by IS2) m^3/min, respectively, while the CS pattern is performed at rates of 0.025 (denoted by CS1), 0.035 (denoted by CS2) and 0.053 (denoted by CS3) m^3/min, respectively.

3 Results and discussion

3.1 Transient combustion behaviour of carbon in different atmospheres

The thermodynamics of the carbon-oxygen system are first calculated and illustrated in Figure 4(a_1). The combustion reaction of carbon can be divided into complete and incomplete combustion reactions. The coke combustion reaction is a typical gas-solid phase reaction, which

can be described by the gas-solid phase film model. As shown in Figure 4(b_1), under negative pressure in the sintering process, oxygen (O_2) diffuses to the surface of solid carbon particles, and then the combustion reaction occurs, resulting in a layer of CO film around the carbon particles and outward diffusion. Subsequently, at high oxygen potential, most of CO is further oxidized by O_2 to generate CO_2 and form a flame surface. In a word, coke combustion efficiency depends on the diffusion rate and heat transfer rate.

What if steam is introduced into the carbon-oxygen system? Figure 4(a_2) shows the thermodynamic results. Although O_2 is sufficient in the sintering process, it is difficult to reach the surface of the coke, so the reducing atmosphere dominates around the coke. Given that steam diffuses more rapidly over the carbon surface than O_2 [70], the steam can promote carbon combustion through the reaction of $C+H_2O=CO+H_2$, and the produced CO is then oxidized to CO_2, resulting in a reduction in CO emissions. Moreover, since the reactions of $CO+H_2O=CO_2+H_2$ and $CO+H_2=C+H_2O$ cannot spontaneously generate at temperatures higher than 820 °C and 680 °C, it is not the decisive pathway for reducing CO emissions. In addition, Figure 4(b_2) schematically shows how the spraying steam affects the carbon combustion reaction in the

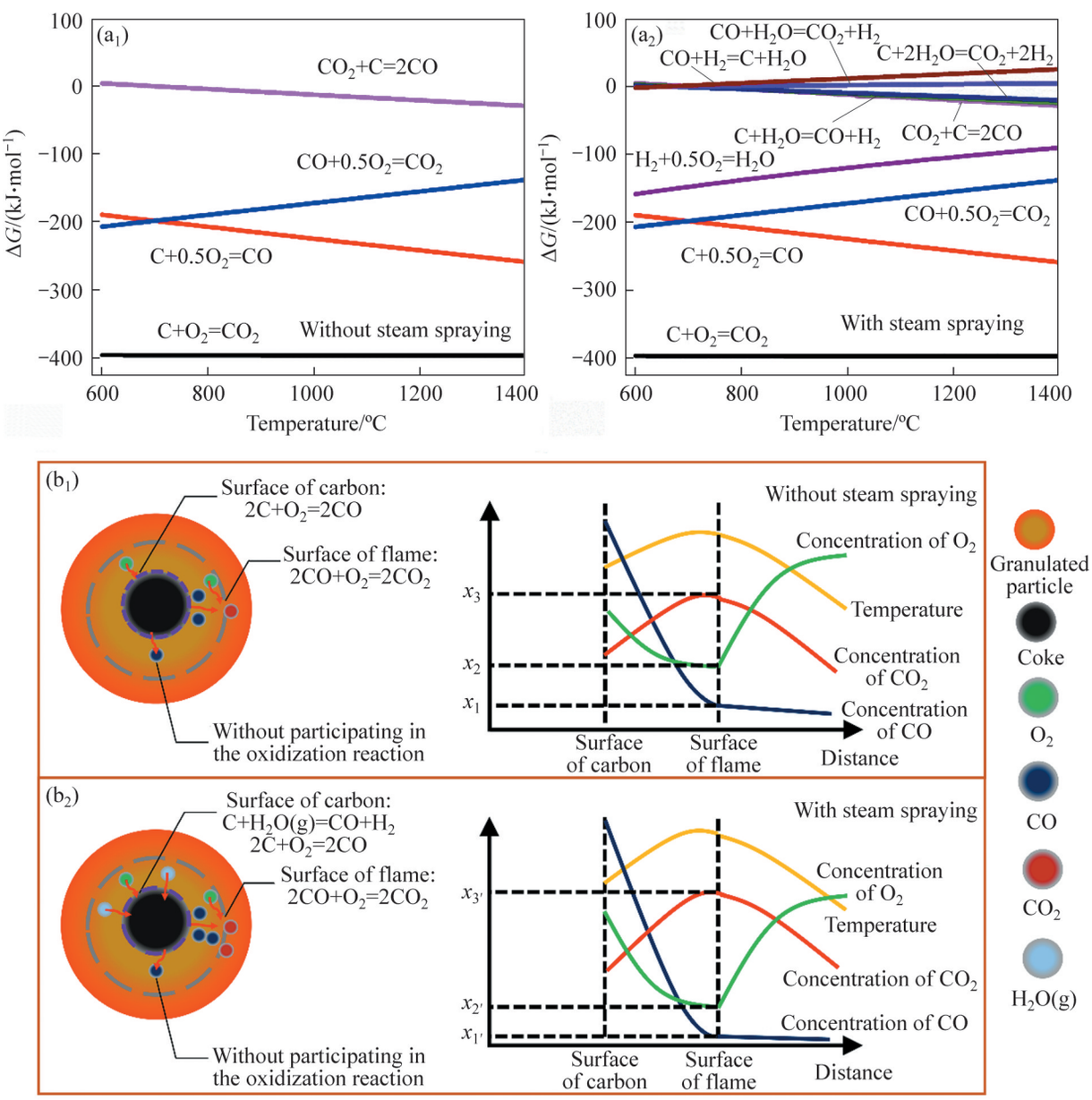

Figure 4 Without steam spraying (a_1, b_1) and with steam (a_2, b_2) spraying: (a_1, a_2)Thermodynamic analysis of carbon-oxygen combustion system; (b_1, b_2) Schematic diagrams of carbon combustion reaction process

sintering process. Due to the reaction of $C+H_2O=CO+H_2$, the CO concentration on the carbon surface should be higher than that without steam spraying. On the one hand, vapor with a larger heat capacity, lower density and kinematic viscosity, can improve the radiation heat transfer capability of gas [71]. On the other hand, the reaction of $C+H_2O=CO+H_2$ can expand the porosity of the coke breeze and further increase the contact area of the carbon-oxygen reaction [72]. Therefore, the introduction of steam provides a beneficial kinetic condition for carbon combustion.

The weight loss curve of the thermogravimetric analysis experiment and the exhaust gas composition are shown in Figure 5. Figure 5(a) shows that the carbon combustion reaction begins at 500 ℃ and completes at approximately 830 ℃. The mass loss in air and air-steam mixed atmosphere is 5.7 mg and 5.9 mg, respectively, and the corresponding mass loss ratios are 80.3% and 83.1%, respectively. In addition, compared with the

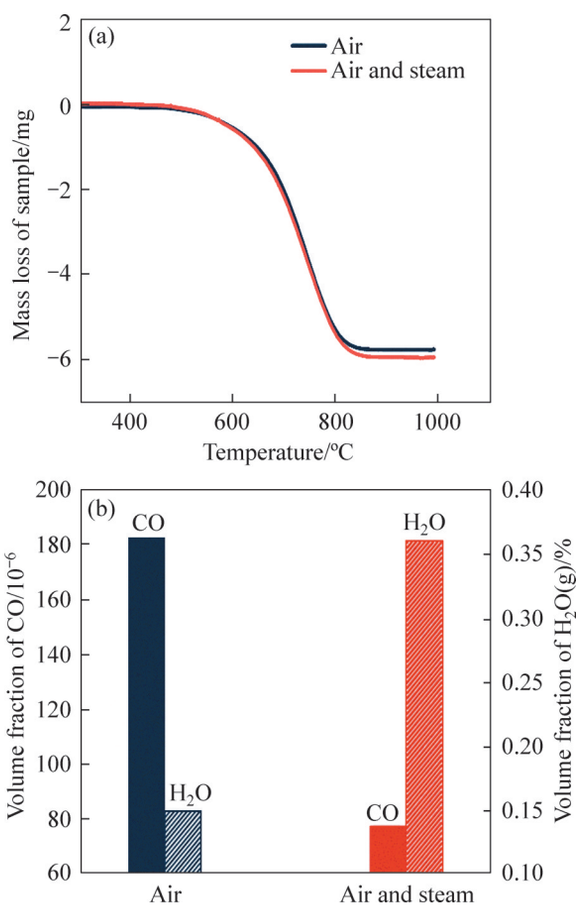

Figure 5 (a) Mass loss curve and (b) CO and H_2O(g) concentrations in the exhaust gas of coke combustion in air and air-steam mixed atmosphere

results in the air atmosphere, the volume fraction of CO in the exhaust gas decreases from 183×10^{-6} to 78×10^{-6} in the humidified air atmosphere, and the volume fraction of vapor increases from 0.15% to 0.36%. Increased mass loss and reduced CO concentration in exhaust gas confirm that steam can improve overall reactivity and reduce CO emissions.

3.2 Transient emission characteristics of carbon combustion after spraying steam in IS pattern

It is generally agreed that at a temperature above 727 ℃, CO is the main product formed at the coke-gas interface [73], and the local temperature in the sintering bed can reach 727 ℃ rapidly. At the coke surface, carbon is first oxidized to CO, and the formed CO is further oxidized to CO_2. O_2 concentration is a key factor in CO oxidation, which determines the efficiency of carbon combustion. The ratio of CO_2 concentration to (CO_2+CO) concentration is generally used as an indicator of combustion efficiency [74−75], which is defined as η in this paper.

Figure 6 compares the temporal gas composition in the exhaust gas of the sintering process operated by the IS pattern. As shown in Figure 6(a), the introduction of steam influences the local O_2 concentration to some extent. First, the entire sintering process is shortened, which is demonstrated by the progress of the time when the concentration of O_2 reaches 21%. Second, taking the IS2 case as an example, it can be found that the concentration of O_2 shows a decreasing trend after each steam spraying operation, while it will increase rapidly once the spraying operation is stopped. However, due to the lower steam volume rate for spraying in the case of IS1, it does not have the same phenomenon. Figures 6(b) and (c) show the temporal concentrations of CO and CO_2 in the exhaust gas. On the one hand, the steam spraying operation decreases the CO concentration but increases the CO_2 concentration. On the other hand, a greater reduction in CO concentration is noticed with a greater amount of spraying. Figure 6(d) further demonstrates that the efficiency of carbon combustion is obviously improved with steam spraying. In addition, average CO concentration and total CO emissions V_{CO} (based on Eq. (1)) in the

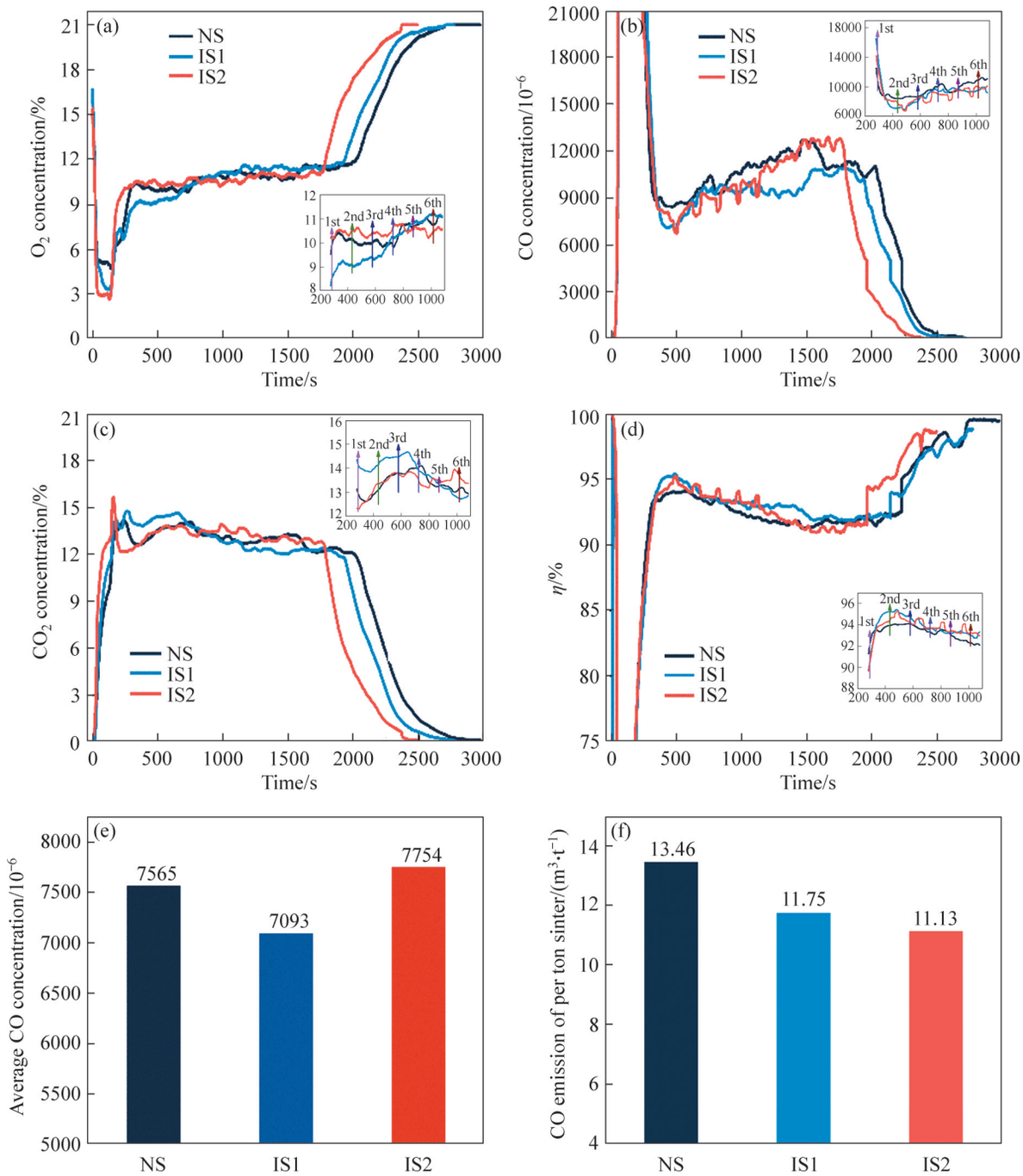

Figure 6 Concentrations profiles in exhaust gas, combustion efficiency distribution and comparative results of CO emissions under IS operations: (a) O_2 concentration distribution; (b) CO concentration distribution; (c) CO_2 concentration distribution; (d) Carbon combustion efficiency distribution; (e) Average CO concentration in the whole sintering process; (f) CO emissions of per ton sinter

sintering process are compared in Figures 6(e) and (f).

$$V_{CO} = Q\int_{t_2}^{t_1} \rho_{CO}\,dt \tag{1}$$

where Q is the flow rate of gas, m^3/h; t_1 and t_2 are the starting time and ending time of sintering, s; ρ_{CO} is the concentration of CO in the exhaust gas.

Although the average CO concentration in IS2 case is higher than in the NS case, total CO emissions for ton sinter are 0.18 m^3/t less than that in the NS case due to shorter sintering duration. Accordingly, CO emissions in IS1 and IS2 cases are 11.75 m^3/t and 11.13 m^3/t, respectively, with a

decrease of 12.70% and 17.30% compared with the NS case.

The transient temperature profiles of the exhaust gas under IS operations are compared with the NS case in Figure 7. It should be noted that the IS2 operation has little effect on the maximum exhaust gas temperature, but the period to reach the maximum temperature is shortened from 2688 s to 2385 s. Overall, the IS operation at a steam volume rate of 0.053 m^3/min can not only improve the combustion efficiency of carbon, but also increase the traveling speed of the combustion zone.

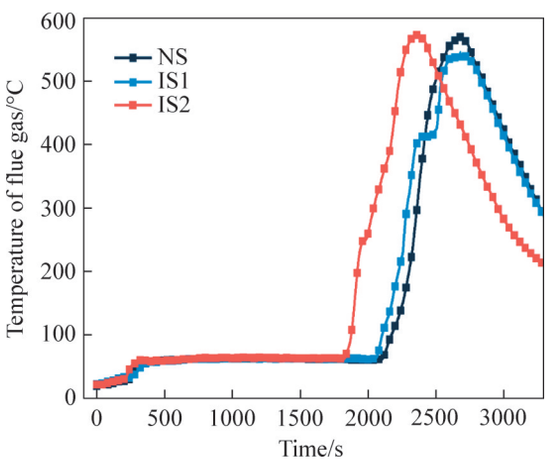

Figure 7 Transient temperature distribution of exhaust gas under IS operations

The influence of IS pattern on the yield and quality of sinter indices is also compared in Figure 8. First, the IS pattern applied in the sintering process produces comparable or even better quality sinters. Specifically, the tumbler indices in NS, IS1, and IS2 cases are 73.6%, 75.6% and 73.2%, respectively. The shatter indices in three cases all exceed 92.9%. Second, productivity showed a clear upward trend, from 82.7% to 84.2% and 84.4%, although sinter yield showed a slight downward trend with a minimum value of 78.8%.

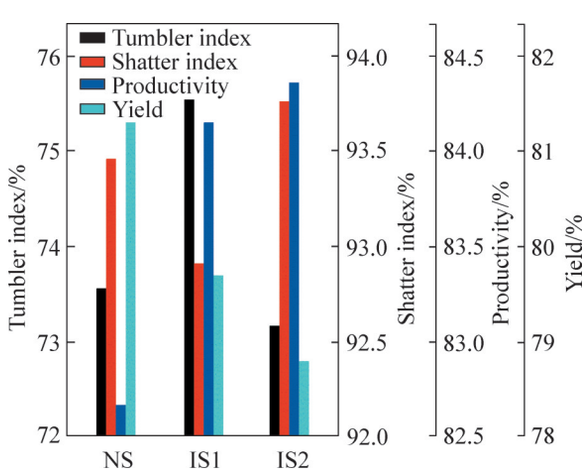

Figure 8 Comparative results of sinter indices under IS operations

3.3 Transient emission characteristics of carbon combustion after spraying steam in CS pattern

Conversely, when sintering pot tests are performed with CS operations as previously explained in Figure 3, the temporal concentrations of O_2, CO and CO_2 in the exhaust gas are compared in Figures 9(a)−(c), respectively, and the corresponding results in the overall spraying process are further compared in the insets. Meanwhile, carbon combustion efficiency, average CO concentration and total CO emissions are compared in Figures 9(d)−(f), respectively.

There are three points worthy of note. First, similar to the IS operation, the temporal O_2 concentration under the CS operation is also lower than the NS case, especially in the period before 600 s. In addition, O_2 concentrations during spraying duration in CS cases are lower than those in IS cases, indicating a higher fuel utilization ratio under CS operations. Second, the sprayed steam promotes the oxidation of CO to CO_2, which can be obtained by the greater carbon combustion efficiency during the spraying duration. As a result, CO emissions in CS3 case is reduced by 29.35% compared to NS. Third, at the same steam volume rate, continuous spraying results in a significant reduction of CO compared to IS cases. Taking the steam volume rate of 0.053 m^3/min as an example, CS3 operation reduces the average CO concentration and total CO emissions by 19.64% and 14.56%, respectively, compared with the IS2 case.

The transient temperatures profiles of the exhaust gas in the CS pattern are also compared with the NS case, as shown in Figure 10. The lower steam volume rate under CS operations has the effect of increasing the exhaust gas temperature, while the greater steam flow rate has the effect of reducing the period to reach the maximum temperature. Specifically, compared with the NS case, the maximum temperature of the exhaust gas under the CS1 operation is increased from 570 °C to

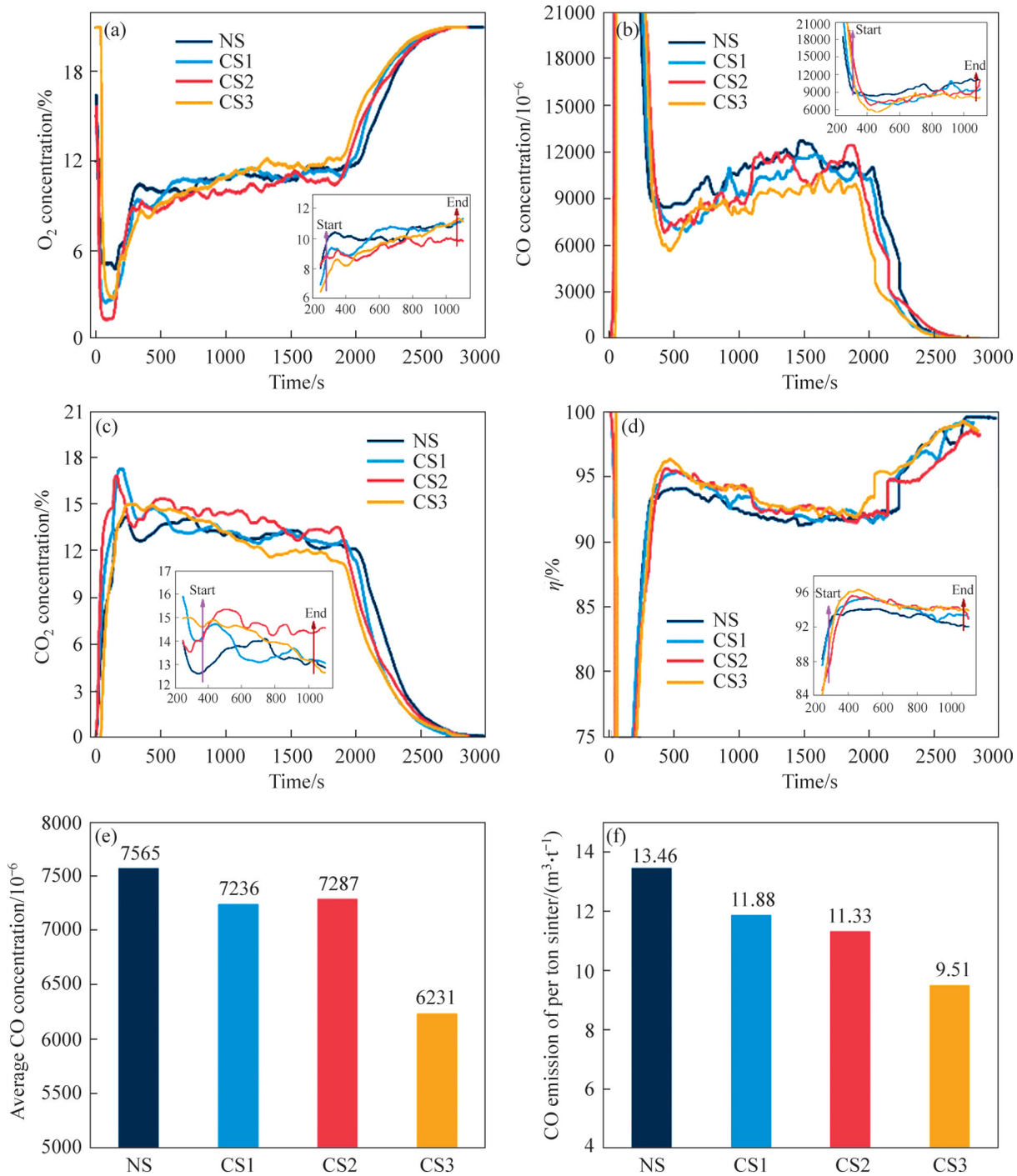

Figure 9 Concentrations profiles in exhaust gas, combustion efficiency distribution and comparative results of CO emissions under CS operations: (a) O_2 concentration distribution; (b) CO concentration distribution; (c) CO_2 concentration distribution; (d) Carbon combustion efficiency distribution; (e) Average CO concentration in the whole sintering process; (f) CO emissions of per ton sinter

617 ℃, while the period to reach the maximum temperature under the CS3 operations is shorten from 2688 s to 2618 s.

The yield and quality of the sinters obtained under CS operations are compared in Figure 11. The introduction of continuous surface steam spraying technology increases the tumbler index and productivity. For example, compared with the NS case, the tumbler index and productivity of the sinters in the CS2 case increase from 73.6% to 74.7% and 82.7% to 84.4%, respectively. In addition, although the shatter index and the sinter

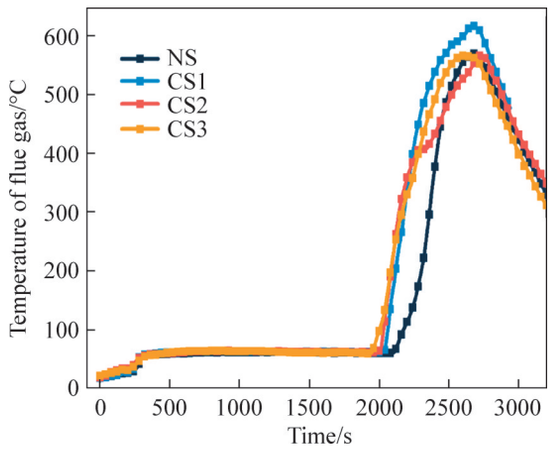

Figure 10 Transient temperature distribution of exhaust gas under CS operations

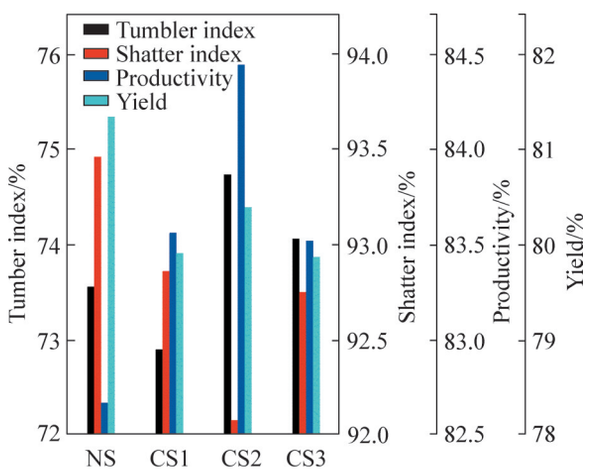

Figure 11 Comparative results of sinter indices under CS operations

yield decrease slightly, they all exceed 92.0% and 79.5%, respectively.

4 Conclusions

This work highlights surface steam spraying technology to improve coke combustion efficiency and thus reduces CO emission in the sintering process. This work not only reveals the mechanisms of intensive carbon combustion in the air-steam mixed atmosphere, but also investigates the influence of IS and CS patterns on sintering performance in terms of temporal exhaust gas composition and sinter productivity and quality indices. The main findings are summarized as follows:

1) The reaction of $C+H_2O=CO+H_2$ and subsequent oxidation of CO play a key role in intensive carbon combustion, further cutting down CO emissions in the air-steam atmosphere.

2) Both the IS and CS patterns can achieve the goal of reducing CO emissions. At the same time, increasing the amount of steam and spraying periods could further reduce the concentration of CO in the exhaust gas. Under the present experimental conditions, continuous steam spraying for 13 min at a volume rate of 0.053 m^3/min is recommended.

3) Once the steam reaches the combustion zone, either O_2 or CO concentration decreases, while the CO_2 concentration increases accordingly, indicating that more CO is oxidized to CO_2. In addition, the introduction of surface steam spraying technology can shorten the sintering period, thus increasing productivity.

4) Compared with NS operation, CO emissions for per ton sinter can be reduced from 13.46 m^3/t to as low as 11.13 m^3/t under IS operation. By contrast, the result can be further reduced to 9.50 m^3/t under CS operation at the same steam volume rate.

Contributors

SUN Cheng-feng conducted the experiments and wrote the initial manuscript. ZHOU Xuan-geng and LI Gang performed the experiments. WANG Yue-fei and XIE Xue-rong provided experimental raw materials. LYU Xue-wei developed the overarching research goals and provided financial support. XU Jian supervised and led the planning and implementation of research activities, and edited the manuscript.

Conflict of interest

SUN Cheng-feng, ZHOU Xuan-geng, LI Gang, WANG Yue-fei, XIE Xue-rong, LYU Xue-wei and XU Jian declare that they have no conflict of interest.

References

[1] WANG Yun-qi, ZHENG He-ran, XIE Zeng-wu, et al. Exploitation of wild Chinese herbs leads to environmental degradation and possible loss of the resource [J]. Environmental Science & Technology, 2012, 46(3): 1307−1308. DOI: 10.1021/es300080p.

[2] CHEN Jie-lin, HUANG Jun-yue, HUANG Xiao-cheng, et al. How does new environmental law affect public environmental protection activities in China? Evidence from structural equation model analysis on legal cognition [J].

Science of the Total Environment, 2020, 714: 136558. DOI: 10.1016/j.scitotenv.2020.136558.

[3] ROSSELOT K, ALLEN D T, KU A Y. Global warming breakeven times for infrastructure construction emissions are underestimated [J]. ACS Sustainable Chemistry & Engineering, 2022, 10(5): 1753 − 1758. DOI: 10.1021/acssuschemeng.1c08253.

[4] XIA Wen-wen, WANG Yong, CHEN Si-yu, et al. Double trouble of air pollution by anthropogenic dust [J]. Environmental Science & Technology, 2022, 56(2): 761 − 769. DOI: 10.1021/acs.est.1c04779.

[5] RUGGERIO C A. Sustainability and sustainable development: A review of principles and definitions [J]. The Science of the Total Environment, 2021, 786: 147481. DOI: 10.1016/j.scitotenv.2021.147481.

[6] LIN Jian-hua, LIN Chang-qing, TAO Ming-hui, et al. Spatial disparity of meteorological impacts on carbon monoxide pollution in China during the COVID-19 lockdown period [J]. ACS Earth and Space Chemistry, 2021, 5(10): 2900 − 2909. DOI: 10.1021/acsearthspacechem.1c00251.

[7] WU Jian, TAL A. From pollution charge to environmental protection tax: A comparative analysis of the potential and limitations of China's new environmental policy initiative [J]. Journal of Comparative Policy Analysis: Research and Practice, 2018, 20(2): 223 − 236. DOI: 10.1080/13876988.2017.1361597.

[8] SHI Jing-xin, HUANG Wen-ping, HAN Hong-jun, et al. Pollution control of wastewater from the coal chemical industry in China: Environmental management policy and technical standards [J]. Renewable and Sustainable Energy Reviews, 2021, 143: 110883. DOI: 10.1016/j.rser.2021.110883.

[9] LU Ya-ling, WANG Yuan, ZHANG Wei, et al. Provincial air pollution responsibility and environmental tax of China based on interregional linkage indicators [J]. Journal of Cleaner Production, 2019, 235: 337 − 347. DOI: 10.1016/j.jclepro.2019.06.293.

[10] ALMETWALLY A A, BIN-JUMAH M, ALLAM A A. Ambient air pollution and its influence on human health and welfare: An overview [J]. Environmental Science and Pollution Research, 2020, 27(20): 24815 − 24830. DOI: 10.1007/s11356-020-09042-2.

[11] LIN Chang-qing, ZHANG Ying-hua. Lofting and circumnavigation of biomass burning aerosols and carbon monoxide from a North American wildfire in October 2020 [J]. ACS Earth and Space Chemistry, 2021, 5(2): 331 − 339. DOI: 10.1021/acsearthspacechem.0c00307.

[12] KUMAR P, KUTTIPPURATH J, von der GATHEN P, et al. The increasing surface ozone and tropospheric ozone in Antarctica and their possible drivers [J]. Environmental Science & Technology, 2021, 55(13): 8542 − 8553. DOI: 10.1021/acs.est.0c08491.

[13] VINAYAGAM N K, HOANG A T, SOLOMON J M, et al. Smart control strategy for effective hydrocarbon and carbon monoxide emission reduction on a conventional diesel engine using the pooled impact of pre-and post-combustion techniques [J]. Journal of Cleaner Production, 2021, 306: 127310. DOI: 10.1016/j.jclepro.2021.127310.

[14] VALENTE O S, da SILVA M J , PASA V M D, et al. Fuel consumption and emissions from a diesel power generator fuelled with castor oil and soybean biodiesel [J]. Fuel, 2010, 89(12): 3637−3642. DOI: 10.1016/j.fuel.2010.07.041.

[15] DEY S, DHAL G C. A review of synthesis, structure and applications in hopcalite catalysts for carbon monoxide oxidation [J]. Aerosol Science and Engineering, 2019, 3(4): 97−131. DOI: 10.1007/s41810-019-00046-1.

[16] ZHANG Wei, WANG Jin-nan, ZHANG Bing, et al. Can China comply with its 12th five-year plan on industrial emissions control: A structural decomposition analysis [J]. Environmental Science & Technology, 2015, 49(8): 4816 − 4824. DOI: 10.1021/es504529x.

[17] ZHANG Qi, XU Jin, WANG Yu-jie, et al. Comprehensive assessment of energy conservation and CO_2 emissions mitigation in China's iron and steel industry based on dynamic material flows [J]. Applied Energy, 2018, 209: 251−265. DOI: 10.1016/j.apenergy.2017.10.084.

[18] TANG Ling, XUE Xiao-da, JIA Min, et al. Iron and steel industry emissions and contribution to the air quality in China [J]. Atmospheric Environment, 2020, 237: 117668. DOI: 10.1016/j.atmosenv.2020.117668.

[19] SUOPAJÄRVI H, UMEKI K, MOUSA E, et al. Use of biomass in integrated steelmaking − Status quo, future needs and comparison to other low-CO_2 steel production technologies [J]. Applied Energy, 2018, 213: 384−407. DOI: 10.1016/j.apenergy.2018.01.060.

[20] de CASTRO J A, da SILVA L M, de MEDEIROS G A, et al. Analysis of a compact iron ore sintering process based on agglomerated biochar and gaseous fuels using a 3D multiphase multicomponent mathematical model [J]. Journal of Materials Research and Technology, 2020, 9(3): 6001 − 6013. DOI: 10.1016/j.jmrt.2020.04.004.

[21] de CASTRO J A, de OLIVEIRA E M, de CAMPOS M F, et al. Analyzing cleaner alternatives of solid and gaseous fuels for iron ore sintering in compacts machines [J]. Journal of Cleaner Production, 2018, 198: 654−661. DOI: 10.1016/j.jclepro.2018.07.082.

[22] LILIK G K, BOEHMAN A L. Advanced diesel combustion of a high cetane number fuel with low hydrocarbon and carbon monoxide emissions [J]. Energy & Fuels, 2011, 25(4): 1444−1456. DOI: 10.1021/ef101653h.

[23] ZHENG Bo, CHEVALLIER F, CIAIS P, et al. Rapid decline in carbon monoxide emissions and export from East Asia between years 2005 and 2016 [J]. Environmental Research Letters, 2018, 13(4): 044007. DOI: 10.1088/1748-9326/aab2b3.

[24] MIRZAJANZADEH M, TABATABAEI M, ARDJMAND M, et al. A novel soluble nano-catalysts in diesel-biodiesel fuel blends to improve diesel engines performance and reduce exhaust emissions [J]. Fuel, 2015, 139: 374 − 382. DOI: 10.1016/j.fuel.2014.09.008.

[25] GAN Min, JI Zhi-yun, FAN Xiao-hui, et al. Insight into the high proportion application of biomass fuel in iron ore sintering through CO-containing flue gas recirculation [J]. Journal of Cleaner Production, 2019, 232: 1335−1347. DOI: 10.1016/j.jclepro.2019.06.006.

[26] JHA G, SOREN S, MEHTA K D. Life cycle assessment of sintering process for carbon footprint and cost reduction: A comparative study for coke and biomass-derived sintering

process [J]. Journal of Cleaner Production, 2020, 259: 120889. DOI: 10.1016/j.jclepro.2020.120889.

[27] ABREU G C, de CARVALHO J A, da SILVA B E C, et al. Operational and environmental assessment on the use of charcoal iniron ore sinter production [J]. Journal of Cleaner Production, 2015, 101: 387 − 394. DOI: 10.1016/j.jclepro.2015.04.015.

[28] CHENG Zhi-long, TAN Zhou-tuo, GUO Zhi-gang, et al. Recent progress in sustainable and energy-efficient technologies for sinter production in the iron and steel industry [J]. Renewable and Sustainable Energy Reviews, 2020, 131: 110034. DOI: 10.1016/j.rser.2020.110034.

[29] HAN Jun, HUANG Zhi-hang, QIN Lin-bo, et al. Refused derived fuel from municipal solid waste used as an alternative fuel during the iron ore sinter process [J]. Journal of Cleaner Production, 2021, 278: 123594. DOI: 10.1016/j.jclepro.2020.123594.

[30] CHENG Zhi-long, FU Pei, GUO Zhi-gang, et al. CFD prediction of heat/mass transfer in multi-layer sintering process assisted with gaseous fuel injection [J]. International Communications in Heat and Mass Transfer, 2021, 128: 105654. DOI: 10.1016/j.icheatmasstransfer.2021.105654.

[31] HE Cheng-chi, FENG Yan-hui, FENG Dai-li, et al. Exergy analysis and optimization of sintering process [J]. Steel Research International, 2018, 89(12): 1800065. DOI: 10.1002/srin.201800065.

[32] FAN X, YU Z, GAN M, et al. Flue gas recirculation in iron ore sintering process [J]. Ironmaking & Steelmaking, 2016, 43(6): 403−410. DOI: 10.1179/1743281215y.0000000029.

[33] SHRESTHA S, XU Jin, YU Ai-bing, et al. Numerical simulation of fuel layered distribution iron ore sintering technology [J]. Ironmaking & Steelmaking, 2022, 49(1): 83−100. DOI: 10.1080/03019233.2021.1968259.

[34] LIU Zheng-jian, NIU Le-le, ZHANG Shi-jun, et al. Comprehensive technologies for iron ore sintering with a bed height of 1000 mm to improve sinter quality, enhance productivity and reduce fuel consumption [J]. ISIJ International, 2020, 60(11): 2400 − 2407. DOI: 10.2355/isijinternational.isijint-2020-219.

[35] WANG Dai-jun, WU Sheng-li, LI Chang-xing, et al. Efficient and clean production practice of large-scale sintering machine [J]. ISIJ International, 2013, 53(9): 1665−1672. DOI: 10.2355/isijinternational.53.1665.

[36] ZHANG Y P, ZHANG J L, ZHANG C, et al. Modelling and visual verification of combustion zone transfer in ultra-thick bed sintering process [J]. Ironmaking & Steelmaking, 2017, 44(4): 304−310. DOI: 10.1080/03019233.2016.1210840.

[37] ZHAO Jia-pei, LOO C E, ELLIS B G. Improving energy efficiency in iron ore sintering through segregation: A theoretical investigation [J]. ISIJ International, 2016, 56(7): 1148−1156. DOI: 10.2355/isijinternational.isijint-2015-686.

[38] LU L, ISHIYAMA O. Recent advances in iron ore sintering [J]. Mineral Processing and Extractive Metallurgy, 2016, 125(3): 132−139. DOI: 10.1080/03719553.2016.1165500.

[39] SUN Cheng-feng, YANG Yi-zhang, XU Yang, et al. A visualization method of quantifying carbon combustion energy in the sintering packed bed [J]. ISIJ International, 2021, 61(6): 1801 − 1807. DOI: 10.2355/isijinternational.isijint-2020-700.

[40] JHA G, SOREN S. Study on applicability of biomass in iron ore sintering process [J]. Renewable and Sustainable Energy Reviews, 2017, 80: 399 − 407. DOI: 10.1016/j.rser.2017.05.246.

[41] JHA G, SOREN S, DEO MEHTA K. Partial substitution of coke breeze with biomass and charcoal in metallurgical sintering [J]. Fuel, 2020, 278: 118350. DOI: 10.1016/j.fuel.2020.118350.

[42] MATSUMURA M, YAMAGUCHI Y, HARA M, et al. Improvement of sinter productivity by adding return fine on raw materials after granulation stage [J]. ISIJ International, 2013, 53(1): 34−40. DOI: 10.2355/isijinternational.53.34.

[43] LI Guang-hui, LIU Chen, YU Zheng-wei, et al. Energy saving of composite agglomeration process (CAP) by optimized distribution of pelletized feed [J]. Energies, 2018, 11(9): 2382. DOI: 10.3390/en11092382.

[44] PAL J, GHORAI S, GOSWAMI M C, et al. Development of pellet-sinter composite agglomerate for blast furnace [J]. ISIJ International, 2014, 54(3): 620 − 627. DOI: 10.2355/isijinternational.54.620.

[45] WANG Yao-zu, ZHANG Jian-liang, LIU Zheng-jian, et al. Recent advances and research status in energy conservation of iron ore sintering in China [J]. JOM, 2017, 69(11): 2404−2411. DOI: 10.1007/s11837-017-2587-0.

[46] ZHOU Ming-xi, ZHOU Hao. Flame front propagation and sinter strength properties of permeable sintering bed prepared via enhanced granulation with hydrated lime [J]. Asia-Pacific Journal of Chemical Engineering, 2021, 16(2): 2592. DOI: 10.1002/apj.2592.

[47] LU Li-ming, MANUEL J. Sintering characteristics of iron ore blends containing high proportions of goethitic ores [J]. JOM, 2021, 73(1): 306 − 315. DOI: 10.1007/s11837-020-04477-x.

[48] JI Zhi-yun, FAN Xiao-hui, GAN Min, et al. Assessment on the application of commercial medium-grade charcoal as a substitute for coke breeze in iron ore sintering [J]. Energy & Fuels, 2016, 30(12): 10448 − 10457. DOI: 10.1021/acs.energyfuels.6b01876.

[49] KAWAGUCHI T, HARA M. Utilization of biomass for iron ore sintering [J]. ISIJ International, 2013, 53(9): 1599−1606. DOI: 10.2355/isijinternational.53.1599.

[50] LEGEMZA J, FINDORAK R, FROHLICHOVA M. Utilization of charcoal in the iron-ore sintering process [J]. Scientia Iranica, 2016, 23(3): 990 − 997. DOI: 10.24200/sci.2016.3867.

[51] GAN Min, LV Wei, FAN Xiao-hui, et al. Gasification reaction characteristics between biochar and CO_2 as well as the influence on sintering process [J]. Advances in Materials Science and Engineering, 2017, 2017: 1 − 8. DOI: 10.1155/2017/9404801.

[52] SUN Cheng-feng, MA Pan-shuai, DENG Jun-yi, et al. Intensive reduction of fuel consumption in the sintering process of double-layered fuel segregation with return fines embedding [J]. Fuel, 2023, 332: 125955. DOI: 10.1016/j.fuel.2022.125955.

[53] FAN Xiao-hui, YU Zhi-yuan, GAN Min, et al. Combustion behavior and influence mechanism of CO on iron ore sintering with flue gas recirculation [J]. Journal of Central South University, 2014, 21(6): 2391 − 2396. DOI: 10.1007/

s11771-014-2192-0.

[54] FAN Xiao-hui, WONG G, GAN Min, et al. Establishment of refined sintering flue gas recirculation patterns for gas pollutant reduction and waste heat recycling [J]. Journal of Cleaner Production, 2019, 235: 1549−1558. DOI: 10.1016/j.jclepro.2019.07.003.

[55] WANG Gan, WEN Zhi, LOU Guo-feng, et al. Mathematical modeling of and parametric studies on flue gas recirculation iron ore sintering [J]. Applied Thermal Engineering, 2016, 102: 648−660. DOI: 10.1016/j.applthermaleng.2016.04.018.

[56] ZHANG Xiao-hui, FENG Peng, XU Jia-rui, et al. Numerical research on combining flue gas recirculation sintering and fuel layered distribution sintering in the iron ore sintering process [J]. Energy, 2020, 192: 116660. DOI: 10.1016/j.energy.2019.116660.

[57] ZUO Hai-bin, ZHANG Jian-liang, HU Zheng-wen, et al. Load reduction sintering for increasing productivity and decreasing fuel consumption [J]. International Journal of Minerals, Metallurgy, and Materials, 2013, 20(2): 131−137. DOI: 10.1007/s12613-013-0704-9.

[58] WANG Yao-zu, LIU Zheng-jian, ZHANG Jian-liang, et al. Study of stand-support sintering to achieve high oxygen potential in iron ore sintering to enhance productivity and reduce CO content in exhaust gas [J]. Journal of Cleaner Production, 2020, 252: 119855. DOI: 10.1016/j.jclepro.2019.119855.

[59] HUANG Xiao-xian, FAN Xiao-hui, JI Zhi-yun, et al. Investigation into the characteristics of H_2-rich gas injection over iron ore sintering process: Experiment and modelling [J]. Applied Thermal Engineering, 2019, 157: 113709. DOI: 10.1016/j.applthermaleng.2019.04.119.

[60] GAO Qiang-jian, XIE Jian-feng, ZHANG Ying-yi, et al. Mathematical modeling of natural gas injection in iron ore sintering process and corresponding environmental assessment of CO_2 mitigation [J]. Journal of Cleaner Production, 2022, 332: 130009. DOI: 10.1016/j.jclepro.2021.130009.

[61] CHENG Zhi-long, WANG Jing-yu, WEI Shang-shang, et al. Optimization of gaseous fuel injection for saving energy consumption and improving imbalance of heat distribution in iron ore sintering [J]. Applied Energy, 2017, 207: 230−242. DOI: 10.1016/j.apenergy.2017.06.024.

[62] CHENG Z L, WEI S S, GUO Z G, et al. Visualization study on the methane segregation injection technology in iron ore sintering process [J]. Energy Procedia, 2017, 105: 1461−1466. DOI: 10.1016/j.egypro.2017.03.433.

[63] ZHONG Qiang, LIU Hui-bo, XU Liang-ping, et al. An efficient method for iron ore sintering with high-bed layer: Double-layer sintering [J]. Journal of Iron and Steel Research International, 2021, 28(11): 1366 − 1374. DOI: 10.1007/s42243-021-00576-4.

[64] FAN Xiao-hui, YU Zhi-yuan, GAN Min, et al. Appropriate technology parameters of iron ore sintering process with flue gas recirculation [J]. ISIJ International, 2014, 54(11): 2541−2550. DOI: 10.2355/isijinternational.54.2541.

[65] CONKLIN J C, SZYBIST J P. A highly efficient six-stroke internal combustion engine cycle with water injection for in-cylinder exhaust heat recovery [J]. Energy, 2010, 35(4): 1658−1664. DOI: 10.1016/j.energy.2009.12.012.

[66] GLUSHKOV D O, LYRSHCHIKOV S Y, SHEVYREV S A, et al. Burning properties of slurry based on coal and oil processing waste [J]. Energy & Fuels, 2016, 30(4): 3441−3450. DOI: 10.1021/acs.energyfuels.5b02881.

[67] PRATIONO W, ZHANG Jian, CUI Jian-fang, et al. Influence of inherent moisture on the ignition and combustion of wet Victorian brown coal in air-firing and oxy-fuel modes: Part 1: The volatile ignition and flame propagation [J]. Fuel Processing Technology, 2015, 138: 670−679. DOI: 10.1016/j.fuproc.2015.07.008.

[68] XU Jian, QIAO Li. Mathematical modeling of coal gasification processes in a well-stirred reactor: Effects of devolatilization and moisture content [J]. Energy & Fuels, 2012, 26(9): 5759−5768. DOI: 10.1021/ef3008745.

[69] de PAEPE W, SAYAD P, BRAM S, et al. Experimental investigation of the effect of steam dilution on the combustion of methane for humidified micro gas turbine applications [J]. Combustion Science and Technology, 2016, 188(8): 1199−1219. DOI: 10.1080/00102202.2016.1174116.

[70] WANG Lin, LIU Zhao-hui, CHEN Sheng, et al. Physical and chemical effects of CO_2 and H_2O additives on counterflow diffusion flame burning methane [J]. Energy & Fuels, 2013, 27(12): 7602−7611. DOI: 10.1021/ef401559r.

[71] CHEN Xu-ling, HUANG Yun-song, GAN Min, et al. Effect of $H_2O_{(g)}$ content in circulating flue gas on iron ore sintering with flue gas recirculation [J]. Journal of Iron and Steel Research, International, 2015, 22(12): 1107−1112. DOI: 10.1016/S1006-706X(15)30119-9.

[72] PEI Yuan-dong, XIONG Jun, WU Sheng-li, et al. Research and application of sintering surface steam spraying technology for energy saving and quality improvement [C]// TMS Annual Meeting & Exhibition. Cham: Springer, 2018: 785−796.10.1007/978-3-319-72138-5_75.

[73] CHENG Zhi-long, YANG Jian, ZHOU Lang, et al. Experimental study of commercial charcoal as alternative fuel for coke breeze in iron ore sintering process [J]. Energy Conversion and Management, 2016, 125: 254−263. DOI: 10.1016/j.enconman.2016.06.074.

[74] ZHOU Hao, LIU Zi-hao, CHENG Ming, et al. Influence of coke combustion on NO_x emission during iron ore sintering [J]. Energy & Fuels, 2015, 29(2): 974−984. DOI: 10.1021/ef502524y.

[75] ZHOU Ming-xi, ZHOU Hao, CHENG Yi, et al. Investigation on the combustion behaviors of coke and biomass char in quasi-granule with CuO − CeO_2 catalysts in iron ore sintering [J]. Journal of the Energy Institute, 2020, 93(5): 1934−1941. DOI: 10.1016/j.joei.2020.04.008.

(Edited by YANG Hua)

中文导读

蒸汽喷吹烧结填充床强化碳燃烧：减少一氧化碳排放的实验研究

摘要：提高固体燃料的燃烧效率对减少铁矿石烧结过程中的一氧化碳排放具有重要意义。本研究借助蒸汽对焦炭燃烧的辅助作用，在烧结过程中引入表面蒸汽喷吹技术，并验证了该技术在降低一氧化碳排放方面的潜力。首先，在空气与空气-蒸汽混合气氛中分别进行焦炭的热重实验。结果表明，相比于空气气氛，引入蒸汽后的混合气氛可使燃烧废气中的一氧化碳浓度从183×10^{-6}降低到78×10^{-6}。此外，从热力学和动力学角度分析了表面蒸汽喷吹技术减少一氧化碳排放的机理。然后，在无喷吹、间隔喷吹与连续喷吹操作下，进行了一系列实验室规模下的烧结杯试验。结果表明，间隔喷吹和连续喷吹均可降低烧结过程中的一氧化碳排放。在本试验条件下，蒸汽喷吹的最佳方式为以0.053 m^3/min的喷吹流量连续喷吹13 min。与无喷吹案例相比，烧结废气中一氧化碳的平均浓度从7565×10^{-6}降低到6231×10^{-6}，烧结矿的一氧化碳总排放量则从13.46 m^3/t降低到9.51 m^3/t。

关键词：烧结；碳燃烧；蒸汽喷吹；一氧化碳；减排